Measurement 42 (2009) 978–988

Contents lists available at ScienceDirect

Measurement

journal homepage: www.elsevier.com/locate/measurement

Development of a wearable sensor system for quantitative gait analysis

Tao Liu *, Yoshio Inoue, Kyoko Shibata

Department of Intelligent Mechanical Systems Engineering, Kochi University of Technology, 185 Miyanokuchi, Tosayamada-cho, Kami-city, Kochi 782-8502, Japan

ARTICLE INFO

Article history:
Received 10 July 2007
Received in revised form 17 July 2008
Accepted 16 February 2009
Available online 23 February 2009

Keywords:
Quantitative gait analysis
Wearable sensor system
Gait phases

ABSTRACT

This paper presents a study on development of a wearable sensor system for quantitative gait analysis using inertial sensors of gyroscopes and accelerometers. This system was designed to detect gait phases including initial contact, loading response, mid stance, terminal stance, pre swing, initial swing, mid swing and terminal swing, which is quite inexpensive compared with conventional 3D motion analysis systems based on high-speed cameras. Since conventional camera-based systems require costly devices, vast space as well as time-consuming calibration experiments, the wearable sensor-based system is much cheaper. Gyroscopes (ENC-05EB) and two-axis ADXL202 accelerometers are incorporated in this wearable sensor system. The former are attached on the surface of the foot, shank and thigh to measure the angular velocity of each segment, and the latter are used to measure inclination of the attached leg segment (shank) in every single human motion cycle for recalibration. The gyroscope is sensitive to a temperature change or small changes in the structure (mechanical wear), which leads to fluctuating offsets from sensor output in applications of human motion measurements. The orientation estimation algorithm here continuously corrects orientation estimates obtained by mathematical integration of the angular velocity measured using the gyroscopes. Correction is performed using an inclination estimation obtained using the signal of the two-axis accelerometer during the interval of mid stance in each stride. The average of root mean squared error (RMSE) was not over 5.0° (the thigh angle orientation) when the calibration was implemented. Correlation coefficient (R) approached 0.9 when the segment angles obtained from the wearable sensor system were compared with the results from a conventional optical motion analysis system.

1. Introduction

1.1. Research background

The standard method for human motion analysis is optical motion analysis using high-speed cameras to capture human motion. The integration of three-dimensional motion measurement using multi-camera systems and reaction force measurement using force plates has been successfully developed to tracking human body parts and performing dynamics analysis of their physical behaviors in a complex environment [1,2]. However, the optical motion analysis method needs considerable work space and high-speed graphic signal processing devices, and using this analysis method, the devices are expensive, and pre-calibration experiments and off-line analysis of recorded pictures are especially complex and time consuming. Therefore, this method and the other standard systems using magnetic or sonic technologies are limited to laboratory research, and are difficult to be applied in daily life applications or complex environments. Moreover, the human body is composed of many highly flexible segments, and the upper-body motion of human is especially complicated in terms of accuracy calculations.

Thus, wearable sensor system with properties of lower cost, friendly operation and less effect to human is becoming an important topic in biomechanics and clinical applications.

* Corresponding author. Tel./fax: +81 887 57 2170.
E-mail address: liu.tao@kochi-tech.ac.jp (T. Liu).

0263-2241/$ - see front matter © 2009 Elsevier Ltd. All rights reserved.
doi:10.1016/j.measurement.2009.02.002

To implement home-based rehabilitation and tele-rehabilitation, some researchers have developed many kinds of wearable (body-fixed) sensor system based to single accelerometers or multi-accelerometer and gyroscope combinations [3–6]. Moreover, for monitoring activities of daily living of disabled person and providing life support, new techniques using different types of ambulatory sensor systems can be helpful outside of a laboratory [7–10].

Recent research on wearable sensor systems for biomedical applications can be divided into two major directions: one is about state recognition on daily physical activities including walking feature assessment [11,12], walking condition classification [13–16] and gait phase detection [17–20], in which the kinematic data obtained from inertial sensors (accelerometer or gyroscope) are directly used as inputs of some inference techniques; and another direction is for accurate measurement of human motion such as joint angle, body segment 3D position and orientation, in which measurement calibration and data fusing of different inertial sensors are important to decrease errors of the quantitative human motion analysis. In our research, a wearable sensor system for human motion and ground reaction force measurement will be developed to estimate joint moment and muscle tension force, so we are focusing on the second direction for quantitative human motion analysis. There are growing interests in adopting commercial products of 3D motion sensor system, for example, smart sensor module MTx (Xsens, The Netherlands) [21] that realized a motion sensor by three angular rate sensors three accelerometers and three magnetic sensors, can reconstruct tri-axial angular displacements by means of a dedicated algorithm. However, it is sensitive to effect of magnetic filed environment, and the dynamic accuracy of this sensor is two degree RMS which depends on type of motion conditions.

Using accelerometer and gyroscope combination without magnetic sensors, Dejnabadi et al., Williamson et al. and Favre et al. introduced some methods to estimate absolute joint angles without hindrance to natural activities [22–24]; however, segment orientation or joint position is very important information for some human dynamics analysis applications like joint moment estimation [25]. Sabatini et al. as well other authors (Luinge et al.) have proposed algorithms based to strap-down integration for foot orientation estimation by considering inclination during stance phase as initial condition for the integration of angular velocity [26–29]. Dejnabadi et al. also presented a method in [30] to estimate lower limbs orientations using a combination of accelerometers and gyroscopes, in which virtual sensors [22] were used to estimate joint angles, then by fusing the data of accelerometers regarded as goniometers during lower body motion acceleration, stable and drift-free estimation of segment orientation was implemented. As all the authors stated, there is a need of cycle rectification from data of accelerometer for strap-down integration method based to gyroscope measurement, but because of lower precision of accelerometer in dynamic condition and some special application like measurement for paralytic patient where the heel may never contact the ground, cyclically using of data of accelerometer in dynamic condition may be difficult to decrease error during orientation estimation. Some regression networks algorithms were introduced in [31,32] as another resolution for predicting the segmental orientations using wearable measurement devices such as gyroscopes and accelerometers, and the effect of loss of sensor data on lower limbs kinematics prediction was addressed.

In this paper, based on the precision measurement of accelerometer during static situation and a linear regression method for simplified assessment of drift error, we proposed a motion analysis system with intelligent calibration for quantitative gait analysis including gait phase detection and leg segment orientation estimation. This motion analysis system is the combination of three gyroscopes that measure the rotational velocity of the foot, shank and thigh, and a two-axis accelerometer that can detect angle of inclination from measurements of two-directional accelerations projected by gravity acceleration. An error estimation algorithm based on results of direct digital integration of gyroscope signals and segment angles of inclination measured by accelerometer in the static states of human walking, was developed to continuously correct orientation estimates obtained by mathematical integration of the angular velocity measured using gyroscopes. Gait analysis results including leg segment orientation obtained with this motion analysis system were compared with the motion analysis results obtained using a commercial optical motion analysis system.

1.2. Introduction of gait phase

In the past it has been the custom to use normal events as the critical actions separating gait phases. While this practice proved appropriate for the amputee, it often failed to accommodate the gait deviations of patients impaired by paralysis or arthritis. For example, the onset of stance customarily has been called heel strike [18,19]; yet the heel of a paralytic patient may never contact the ground or do so much later in the gait cycle. Similarly initial floor contact may be by the whole foot (foot flat), rather than having forefoot contact occur later, after a period of heel-only support. To avoid these difficulties and other areas of confusion, the Rancho Los Amigos gait analysis committee developed a generic terminology for the functional phases of gait [33].

Analysis of human walking pattern by phases more directly identifies the functional significance of the different motions accruing at the individual joints and segments. In this paper, a normal walking gait cycle is divided into eight different gait phases including initial contact, loading response, mid stance, terminal stance, pre-swing, initial swing, mid swing and terminal swing (as shown in Fig. 1) [34].

In the following discussion, we assume that the subjects are viewed from the right lateral side and anticlockwise rotations are considered positive. θ_f, θ_s and θ_t represent the inclination angles of the foot, shank and thigh with respect to gravity direction, respectively. ω_f, ω_s and ω_t represent the angular velocities of the foot, shank and thigh in the lateral plane, respectively. Finally, $\varepsilon_\theta, \varepsilon_\omega$ and ε_a represent small threshold values for the detection of close to zero angle displacements, angular velocities and accelerations, respectively.

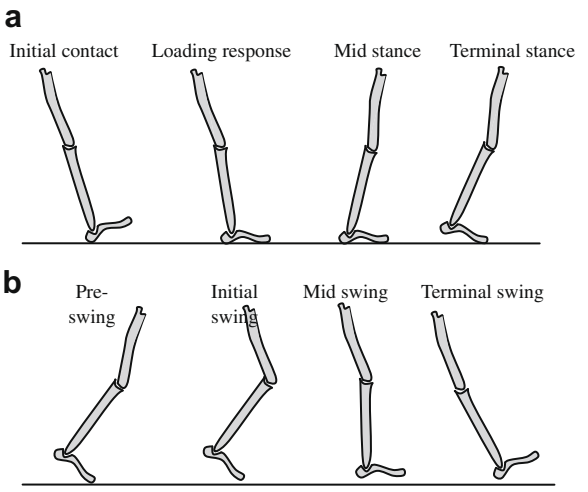

Fig. 1. (a) Gait phases of stance period. (b) Gait phases of swing period. Each of the eight gait phase has a functional objective and a critical pattern of selective synergistic motion to accomplish this goal. The sequential combination of the phases also enables the lime to accomplish three basic tasks, which include weight acceptance, single limb support and limb advancement. Weight acceptance begins the stance period and uses phases of initial contact and loading response. Single limb support continues stance with phases of mid stance and terminal stance. Limb advancement begins in phase of pre-swing and then continues through the three phases of initial swing, mid swing and terminal swing.

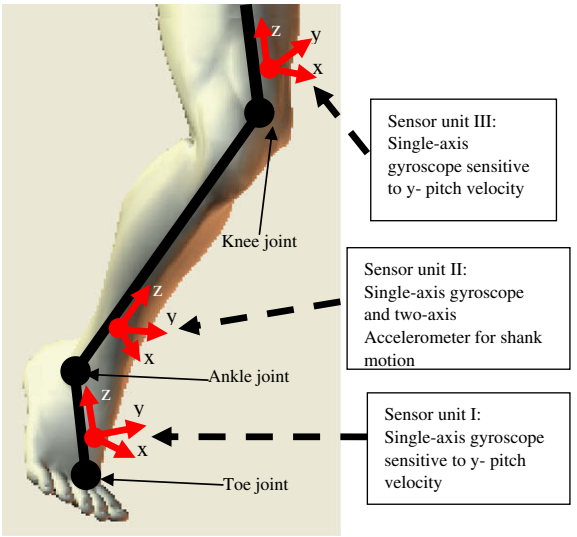

Fig. 2. Position and coordinates of the sensor units. In the local orientation coordinate of the sensor unit (*X*-, *Y*- and *Z*-axis), *Y*-axis denotes each joint's rocker axis, which is parallel to the sensitive axis of the gyroscope, while *X*-axis and *Z*-axis denote the unity vectors in the radial and tangential direction, respectively.

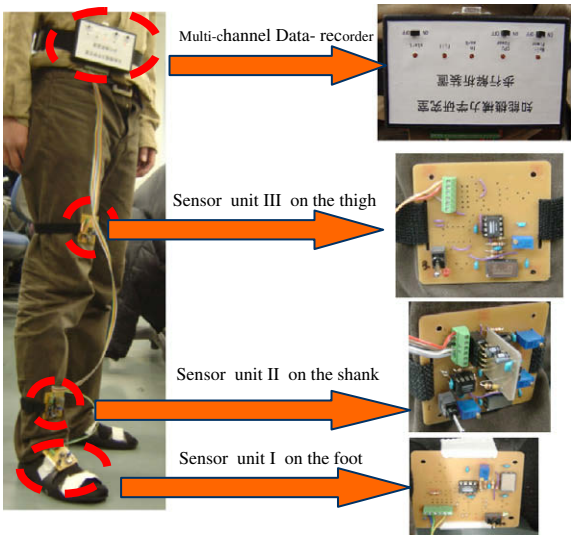

Fig. 3. Hardware system of the sensor system. A strap system is designed for the binding between the sensor units and human body. The sensor unit is attached to the strap. During walking, the strap is tied around the limb to secure the position of the sensor unit.

2. Methods and materials

2.1. Sensor system

As shown in Fig. 2, three gyroscopes are used to measure angular velocities of leg segments of foot, shank and thigh (ω_1, ω_2 and ω_3). The sensing axis is vertical to the medial–lateral plane so that the angular velocity in the sagittal plane can be detected. In local coordinates of three segments, sensing axis of the gyroscopes is along *y*-axis, and the *z*-axis is along leg-bone. A two-axis accelerometer is attached on the side of shank to measure two-directional accelerations along tangent direction of *x*-axis (a_t) and sagittal direction of *z*-axis (a_r). In this system, the data from accelerometer are fused with data collected from gyroscopes for cycle system calibration, through supplying initial angular displacement of the attached leg segment.

2.2. Hardware system design

As shown in Fig. 3, the wearable sensor system includes an eight-channel data recorder (size, 110 mm × 60 mm × 20 mm; weight including cables, 200 g), a gyroscope and accelerometer combination unit and two gyroscope units. The two gyroscope units are attached on foot and thigh, respectively, and the gyroscope and accelerometer combination unit is located on shank, which is near to ankle. The data recorder can be pocketed by the subject. The principle operation of the gyroscope is the measurement of the Coriolis acceleration, which is generated when a rotational angular velocity is applied to the oscillating piezoelectric bimorph. These inertial sensor can work under low energy consumption (4.6 mA at 5 V), and are appropriate for ambulatory measurements. The signal from the gyroscopes and accelerometer is amplified and low-pass filtered (cutoff frequency: 25 Hz) to remove electronic noise. The frequencies outside the pass band are filtered out because they are invalid in study of human kinetics.

The multi-channel data recorder is specially designed for the wearable sensor system. A micro-computer PIC (16F877A) is used to develop the pocketed data recorder, and sampling data from the inertial sensors can be saved

in a SRAM. An off-line motion analysis can be performed by feeding data saved in the SRAM to a personal computer through a RS232 communication module or a wireless module. Since gyroscope (ENC-03J), accelerometer-chip (ADXL202) and PIC system are all devices of low energy consumption, the wearable sensor system can be powered using a rechargeable battery of 300 mAh (NiMH 30R7H).

2.3. Calibration of sensor units

Complete architecture of a calibration system is showed in Fig. 4(a), and hardware devices of the system mainly include A/D card (Keyence NR-110), a potentiometer, a reference angle finder and a clamp (Fig. 4(b)).

The sensor units are calibrated in two states of static and dynamic. The calibration of the accelerometer sensor is carried out during the static state. The accelerometer in sensor unit is subjected to different gravity vectors by rotating a based axis which is connected with a potentiometer. The dynamic calibration is completed to calibrate the gyroscopes and test the accelerometer in a moving condition. In both cases the calibration matrixes are computed using the least squares method.

$[C_\theta]$ is calibration matrix for the angle position (1), where $[\theta]$ is the matrix of the imposed quantities, which

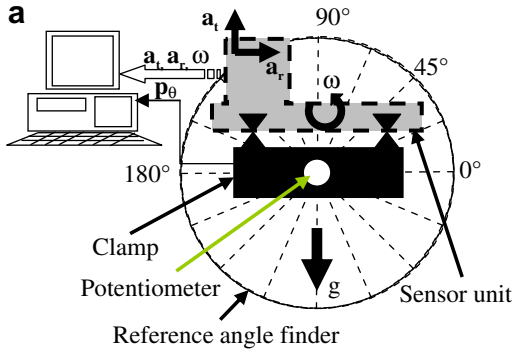

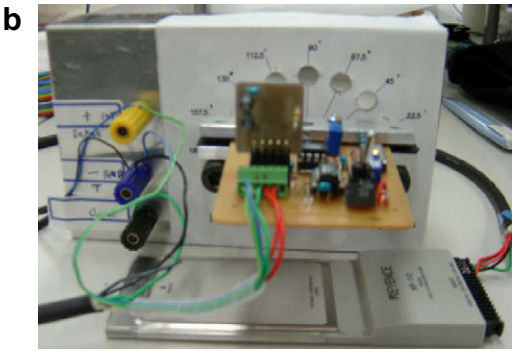

Fig. 4. (a) Architecture of the equipment for the calibration of the sensor unit. Two-axis accelerometer is used to measure two-directional accelerations of a_t and a_r, and p_θ is output signal of the potentiometer which measures imposed rotational quantities and provides reference angular velocity quantities through difference computing. Signal of gyroscope in the sensor unit is defined as ω, and its positive direction is anticlockwise. The four signals of p_θ, ω, a_t and $a_r$are sampled into computer through a 12-bit A/D card. (b) Hardware devices with mechanical case and interface for the calibration of the sensor unit.

Table 1
Calibration data of a sensor unit.

Angle finder	Potentiometer	Accelerometer	
θ (°)	p_θ (V)	a_t (V)	a_r (V)
0	1.438	2.541	3.004
−22.5	1.355	2.798	2.943
−45	1.284	2.985	2.813
−67.5	1.209	3.108	2.602
−90	1.134	3.138	2.369
22.5	1.512	2.294	2.969
45	1.595	2.096	2.849
67.5	1.671	1.937	2.663
90	1.748	1.882	2.457

in this specific case were obtained when the sensor unit is rotated to different positions on the angle finder plane; $[p_\theta]$ is the matrix of the quantities acquired from the potentiometer, in the specific sensor unit positions. Angular position $[\theta_r]$ can be calculated using (2), and angular velocity of the sensor unit is obtained through difference computing of the angular positions in serial time. Gravity g subjected to the two sensitive axis (a_t and a_r) of the accelerometer is estimated in (3) and (4)

$$[C_\theta] = [\theta][p_\theta]^T([p_\theta][p_\theta]^T) - 1 \quad (1)$$

$$[\theta_r] = [C_\theta] \cdot [p_\theta] \quad (2)$$

$$A_t = -g \cdot \cos(\theta_r) \quad (3)$$

$$A_r = -g \cdot \sin(\theta_r) \quad (4)$$

$[C_{at}]$ and $[C_{ar}]$ are calibration matrixes for the two-axis accelerometer (5) and (6), where $[A_t]$ and $[A_r]$ are the matrixes of the imposed quantities, which in this specific case were obtained when the sensor unit is subjected to different g vectors by rotating the sensor unit on the angle finder plane; $[a_t]$ and $[a_r]$ are the matrixes of the quantities assessed by the accelerometer in the sensor unit. Eqs. (7) and (8) give summations of subjected gravity g and segment motion acceleration on the two sensitive axes using the output signals of the accelerometer. Table 1 shows data of a sensor unit from a calibration experiment

$$[C_{at}] = [A_t][a_t]^T([a_t][a_t]^T) - 1 \quad (5)$$

$$[C_{ar}] = [A_r][a_r]^T([a_r][a_r]^T) - 1 \quad (6)$$

$$[A_r^{re}] = [C_{ar}] \cdot [a_r] \quad (7)$$

$$[A_t^{re}] = [C_{at}] \cdot [a_t] \quad (8)$$

$[C_g]$ is calibration matrix for gyroscope sensor in the sensor units (9), where $[V_g]$ and $[p_\theta]$ are the matrixes of the quantities, respectively, acquired from the gyroscope and potentiometer in a serial time (t); $[C_\theta]$ is calibration matrix for the angle position (1). Angular position $[\theta_r]$ can be calculated using (2), and angular velocity of the sensor unit is obtained through difference computing of the angular positions in serial time. Gravity g subjected to the two sensitive axis (a_t and a_r) of the accelerometer is estimated in (3) and (4)

$$[C_g] = [C_\theta][p_\theta]\left[\int V_g dt\right]\left(\left[\int V_g dt\right]\left[\int V_g dt\right]^T\right) - 1 \quad (9)$$

3. Methods: quantitative gait analysis

3.1. Gait phase detection algorithm

In the following discussion, we assume that the subject is viewed from the right lateral side and anticlockwise rotations are considered positive. θ_f, θ_s and θ_t represent the inclination angles of the foot, shank and thigh with respect to gravity direction, respectively. We also define θ_{f0}, θ_{s0} and θ_{t0} as initial (neutral) quantities of the orientation angle. ω_f, ω_s and ω_t represent the angular velocities of the foot, shank and thigh in the lateral plane, respectively. Finally, $\varepsilon_\theta, \varepsilon_\omega$ and ε_a represent small threshold values for the detection of close to zero angle displacements, angular velocities and accelerations, respectively.

A completed (normal) gait cycle is defined as following:

S1: Start of initial contact (end of terminal swing). The hip is flexed, the knee is extended $(\theta_s - \theta_t = \theta_{s0} - \theta_{t0})$, and the ankle is dorsiflexed to neutral $(\theta_f - \theta_s = \theta_{f0} - \theta_{s0})$. The inclinations of the leg segments are obtained by integrating the gyroscopes signal.
Sensor condition: $\omega_f = \varepsilon_\omega, \omega_s = \varepsilon_\omega$ and $\omega_t = \varepsilon_\omega$.
S2: Start of loading response (end of initial contact). Using the heel as a rocker, the knee is flexed for shock absorption $(\theta_s - \theta_t < \theta_{s0} - \theta_{t0}, \theta_s > 0 \text{and} \theta_t > 0)$.
Sensor condition: $\omega_f < 0, \omega_s < 0$ and $\omega_t < 0$.
S3: Start of mid stance (end of loading response). In this phase, the limb advances over the stationary foot by ankle dorsiflexion (ankle rocker) while the knee and hip extend $(\theta_s - \theta_t = \varepsilon_\theta)$.
Sensor condition: $\omega_f = \varepsilon_\omega, \omega_s < 0$ and $\omega_t < 0$.
S4: Start of terminal stance (end of mid stance). The terminal stance begins with heel rise and continues until the other foot strikes the ground, in which the heel rise and the limb advance over the forefoot rocker $(\theta_s - \theta_t = \theta_{s0} - \theta_{t0}, \theta_f < 0, \theta_s < 0$ and $\theta_t < 0)$.
Sensor condition: $\omega_f < 0, \omega_s < 0$ and $\omega_t < 0$.
S5: Start of pre-swing (end of terminal stance). The limb responds with increased ankle plantar flexion $(\theta_f < 0)$, greater knee flexion $(\theta_s - \theta_t < 0)$ and loss of hip extension.
Sensor condition: $\omega_f < 0, \omega_s < 0$ and $\omega_t < 0$.
S6: Start of initial swing (end of pre-swing). In this phase, the foot is lifted and limb advanced by hip flexion and increased knee flexion $(\theta_s - \theta_t < 0)$.
Sensor condition: $\omega_f > 0, \omega_s > 0$ and $\omega_t > 0$.
S7: Start of mid swing (end of initial swing). The knee is allowed to extend in response to gravity while the ankle continues dorsiflexion to neural $(\theta_f - \theta_s < 0, \theta_t > 0$ and $\theta_s < \varepsilon_\theta)$.
Sensor condition: $\omega_f > 0, \omega_s > 0$ and $\omega_t > 0$.
S8: Start of terminal swing (end of mid swing). Limb advancement is completed as the leg (shank) moves ahead of the thigh. In this phase the limb advancement is completed by knee extension, and the hip maintains its earlier flexion $(\theta_f - \theta_s = \theta_{f0} - \theta_{s0})$, and the ankle remains dorsiflexed to neural.
Sensor condition: $\omega_f - \omega_s = \varepsilon_\omega$ and $\omega_t > 0$.

In this paper, the motion analysis system with intelligent calibration for leg segment quantitative leg-motion analysis is developed. According above quantitative assessment of the eight gait phases, if the leg segments' orientations (θ_f, θ_s and θ_t) cannot be accurately obtained and combined with the signals of the sensor units (ω_f, ω_s and ω_t), it is almost impossible that all the gait phases are effectively detected.

3.2. Quantitative gait analysis

The loop frequency of the phase record is 100 Hz, i.e., equal to the sensors sampling frequency, and the number of sampling time point is counted in an integer value i ($i = 1,2,3,\ldots$). The orientation of leg segment $(\theta(i))$ can be calculated by integration of the angular velocity $(\omega(i))$ of leg segment ((9) and (10)), which is directly measured using the wearable sensor unit. The inclination of shank and thigh is set to zero in the initial period, while the inclination of foot is set to 90° at start. However, the gyroscope in the sensor unit is a kind of inertial sensor that is affected by drift errors when it is worn on human body, so the integral calculation in (9) may produce cumulated errors in a multi-step walking motion analysis

$$\theta(i) = \theta(i-1) + (\omega(i-1) + \omega(i))\Delta t/2 \tag{9}$$

where

$$\theta(0) = \theta_0; \quad i = 1,2,3\ldots \tag{10}$$

We define the gait cycle (walking gait cycle number $k = 1,2,\ldots$) as the period from one stance phase of the foot to the next stance phase of one foot. In every walking cycle, the time points of transition from loading response phase to mid stance phase, and transition from pre-swing to initial swing phase are defined as $T_{41}(k), T_{42}(k), T_{43}(k)$ and $T_{44}(k)$, respectively. Based on a pre-analysis of gait phase, the human motion analysis is implemented by calculating body segments' angular displacements using inertial sensors of gyroscopes and accelerometers. As shown in Fig. 5, we can primarily detect the mid stance phase just using gyroscope signals and raw integration results of gyroscope signals from the three sensor units ($\omega_t < 0, \omega_f = \varepsilon_\omega, \omega_s < 0$ and $\theta_s < 0$). Moreover, we find that the rotational angular velocities of the shank and thigh are very small in later interval of this phase, because ankle is in state of dorsiflexion, and shank rotational velocity is limited. Therefore, the accelerometer can be used for inclination measurement with respect to gravity acceleration, when shank's sagittal direction A_r (11) and A_t (12) are mainly affected by the gravity acceleration's projection. Hence, we can make cycle calibration by measuring initial angular orientation of the attached segment (shank) using (13), and foot orientation $(\theta_f^m = 0)$ and thigh orientation $(\theta_t^m = \theta_s^m)$ are the initial calibration quantities for calculation of foot and thigh orientation. Integral calculations are performed in every gait cycle, which can decrease the cumulated errors in the longtime walking experiments

$$A_r = -g \cdot \sin(\theta_s^m) + D \cdot (\omega_s^m)^2 \tag{11}$$

$$A_t = -g \cdot \cos(\theta_s^m) + D\dot{\omega}_s^m \tag{12}$$

$$\theta_s^m = \arctan(A_r/A_t) \tag{13}$$

However, some subjects' (e.g., paralytic patient) the heel may never contact the ground, and the proposed direct inference algorithm cannot be used for cycle recalibration

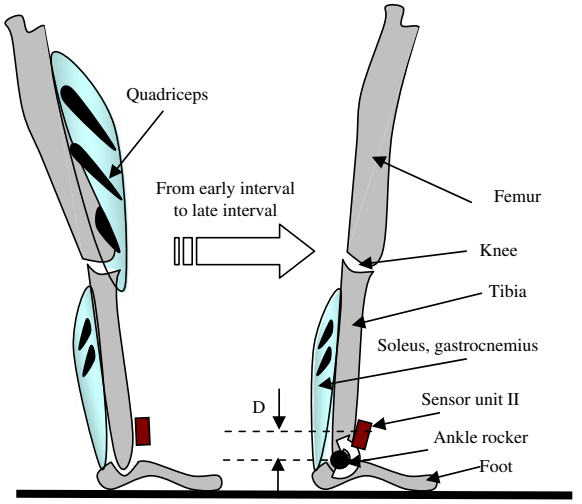

Fig. 5. Mid stance phase including early interval and late interval. The orientation calibration is implemented in late interval of mid stand. Early interval has body over mid foot with climb vertical, ankle neutral and foot flat, in which quadriceps and soleus muscles are in activity. Later interval has body over forefoot with continued heel contact, while ankle is in state of dorsiflexion which limit shank rotational velocity. A small distance between sensor unit II and ankle rocker is denoted using D (it is about 50 mm). Moreover in later interval, soleus and gastrocnemius are only extensor muscles around tibia, which produces least vibration effect on the accelerometer.

to decrease integration error. A linear regression method was developed to calculate drift error coming from digital integration, in which we supposed the error increase in linear function. The summary error $(\theta_e = \theta_i - \theta_m)$ is obtained from single walking test in which subjects are requested to walk along a straight leading line, in which we let θ_i be direct integration results by (9), and θ_m be reference static inclination angle measured using accelerometer by (13). Error estimation function $(\theta_e(i))$ is given as following equation based to linear regression

$$\theta_e(i) = \Delta t \cdot i \cdot (\theta_i - \theta_m)/t, \quad i = 1, 2, 3, \ldots, t \tag{14}$$

$$\theta_c(i) = \theta(i) - \theta_e(i) \tag{15}$$

where Δt is sampling time and $\theta_c(i)$ was defined as estimated angle with error correction. A group of example figures including $\theta(i)$ and $\theta_e(i)$ for foot angle estimation is shown in Fig. 6. Drift error was significantly reduced from the simplified error estimation method; in the next step, the results of leg segment orientation were compared with measurements of a commercial motion analysis system based to high-speed cameras.

3.3. The optical motion analysis system

To validate the sensor system performance we have compared the quantitative results of the sensor system with the measurements obtained with a commercial optical motion analysis system Hi-DCam (NAC Image Technology, Japan). Hi-DCam tracked and measured the three-dimensional (3D) trajectories of retro-reflective markers placed on the subject's body, as shown in Fig. 7. Two high-speed cameras with sampling frequency

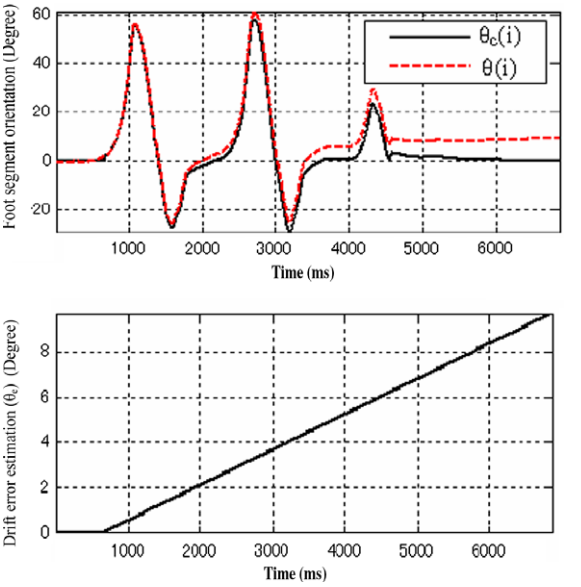

Fig. 6. Example figures of foot segment orientation estimated by eliminating linear drift error.

50 Hz are used to track the marker positions with accuracy of 1 mm.

3.4. Performance analysis of the sensor system

Two criteria are used to evaluate the similarity between results of the sensor system and results of the optical motion analysis system.

1. The motion analysis results of the two systems should be identical in a time domain and therefore the correlation coefficient should approach one.
2. The motion analysis results of the two systems should be quantitatively identical, and therefore the root mean squared error (RMSE) should approach zero.

The correlation coefficient is calculated to compare motion analysis results of the two sensor systems. If the

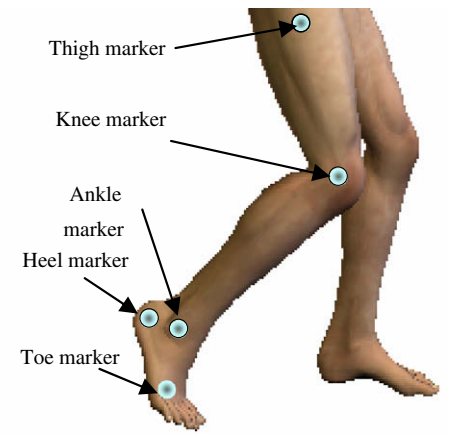

Fig. 7. Positions of the retro-reflective markers.

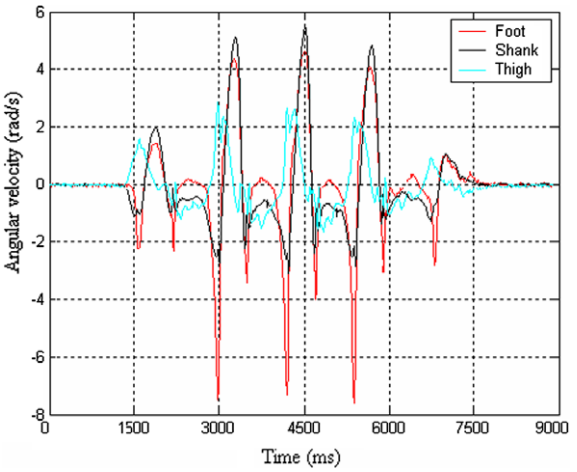

Fig. 8. Signals of the gyroscopes worn on a subject's limb.

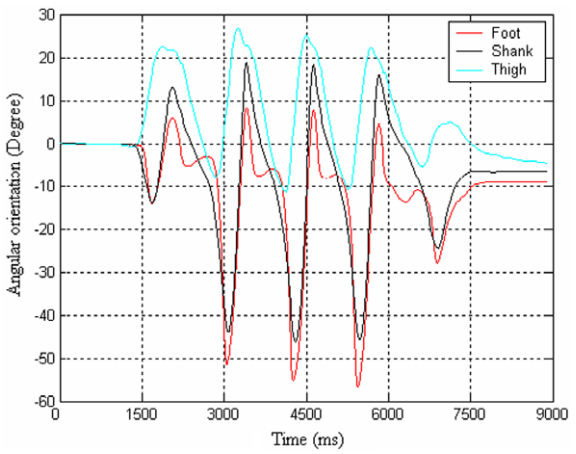

Fig. 9. Estimation results of leg segments' rotational angles.

correlation coefficient has a value closed to +1, then there is a linear relationship between these two results in the time domain. Correlation coefficient (R) is defined as:

$$R = \frac{(n\sum FF_r - \sum F \sum F_r)}{\sqrt{\left(n\sum F^2 - (\sum F)^2\right)\left(n\sum F_r^2 - (\sum F_r)^2\right)}} \quad (16)$$

where F is the results obtained from the developed sensor system, F_r is the results from the reference optical motion analysis system, and the n is the number of the sample data.

Moreover, the root mean squared error (RMSE) is used to compare the closeness in amplitude of the two system's measurement results. The percent error (PE) was calculated as the ratio between the RMSE errors to the average peak-to-peak amplitude of the optical analysis system's measurements

$$\mathrm{RMSE} = \sqrt{\left(\frac{1}{n}\sum (F - F_r)^2\right)} \quad (17)$$

4. Experimental study

The experiment of the sensory system for leg-motion analysis is implemented in the following three steps. First, the sensor devices are worn on the subject's leg to measure 2D motion of the foot, shank and thigh, and the sensors' data are saved in the pocketed data recorder. Second, when the human motion record is finished, the data in the data recorder will be fed into personal computer through serial port (RS232), then leg-motion data is prepared for the off-line motion analysis computing. Finally, the leg-motion analysis is performed to estimate the leg segments' angular orientations.

4.1. Drift effect

As shown in Fig. 8 and Fig. 9, an off-line analysis was made to analyze the leg segments motion during walking, when the subject walked with a stride length about 0.8 m, a gait cycle time about 1.2 s. The experiments data were processed using MATLAB, in which a direct integral calculation was designed to estimate orientations of the three leg segments.

We have completed the motion analysis experiments on 10 subjects (average age, 21; average height, 1.7 m). To test drift error from the gyroscope worn on human body, we have compared the quantitative results of the sensor system using direct integral calculation with the measurements obtained with a commercial optical motion analysis system. As shown in Table 2, the maximum value of RMSE the orientation error during walking experiments

Table 2
RMSE of orientation drift from integral calculation.

	Foot (RMSE)			Shank (RMSE)			Thigh (RMSE)		
	Stride 1	Stride 2	Stride 3	Stride 1	Stride 2	Stride 3	Stride 1	Stride 2	Stride 3
Subject 1	3.7	3.9	4.6	5.0	1.4	8.8	3.9	7.9	1.3
Subject 2	0.1	3.2	8.0	5.4	4.7	8.3	13.2	9.2	10.0
Subject 3	3.1	6.6	9.9	1.6	0.4	3.4	0.5	7.2	14.9
Subject 4	2.4	4.5	5.4	2.5	5.0	2.9	4.8	16.2	14.3
Subject 5	1.3	2.1	1.9	1.9	3.8	6.3	6.4	7.6	0.3
Subject 6	2.2	3.6	3.9	3.1	10.3	6.2	1.8	10.0	5.1
Subject 7	5.4	4.8	4.5	1.1	2.3	0.1	3.8	−6.4	7.4
Subject 8	9.4	8.7	11.6	7.4	4.2	6.3	0.9	−2.8	14.7
Subject 9	0.3	3.8	2.1	6.1	5.4	8.4	13.3	13.5	16.6
Subject 10	4.0	6.3	7.6	3.1	5.0	2.2	4.7	1.5	10.3

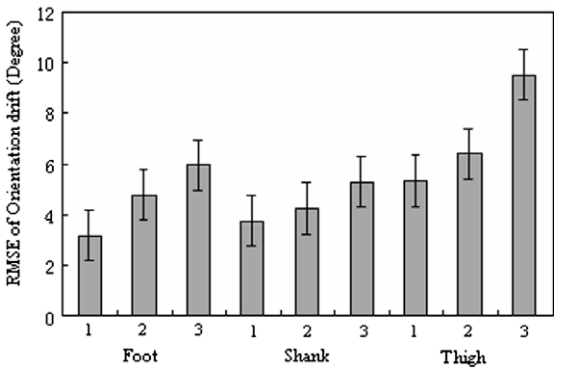

Fig. 10. Average orientation drift error (RMSE value) using direct integral calculation. In the serial three strides the drift of the three segments (foot, shank and thigh) continuously increases when using direct integral calculation from gyroscope signals.

is 16.6° because of effects of drift. In the serial three strides, the drift of the three segments (foot, shank and thigh) continuously increase when using direct integral calculation from gyroscope signals (Fig. 10).

4.2. Intelligent calibration for reducing drift

The mid stance phase can be detected just using gyroscope signals and raw integration results of gyroscope signals from the three sensor units ($\omega_t < 0, \omega_f = \varepsilon_\omega, \omega_s < 0$ and $\theta_s < 0$). Moreover, we find that the rotational angular velocities of the shank and thigh are very small in later interval of this phase, because ankle is in state of dorsiflexion, and shank rotational velocity is limited. Therefore, the accelerometer can be used for inclination measurement with respect to gravity acceleration, when shank's sagittal direction A_r (11) and A_t (12) are mainly affected by the gravity acceleration's projection. Fig. 11 shows a subject walking experiment on period calibration for reducing drifts. In each mid stance phase of the four strides, the angle signals from accelerometer were used as initial value of integral calculation instead of the value from integral signal of the gyroscope (Table 3).

Calibration experiments were finished on a group of subjects using the signals of the wearable sensor system and the optical motion analysis system. As shown in Fig. 12, the shank angle of a subject was derived from our motion analysis system in time domain. The drift

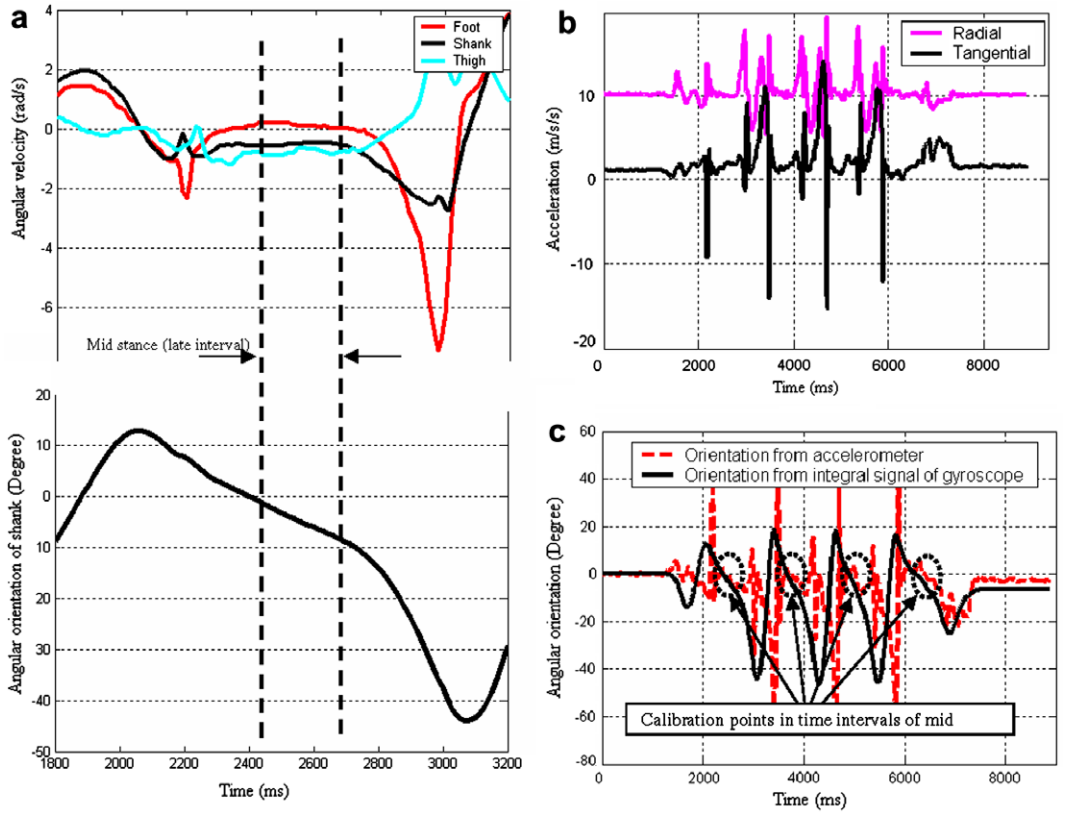

Fig. 11. Period calibration by fusing signals of gyroscopes and accelerometers. (a) Late interval of mid stance in a gait cycle. Mid stance phase can be detected using gyroscopes on low limb: $\omega_t < 0, \omega_f = \varepsilon_\omega, \omega_s < 0$ and $\theta_s < 0$. (b) Signals of accelerometer attached on shank during human walking. In the whole gait cycle, the acceleration measurements include projections of the sum of gravity acceleration and the attached segment motion. The accelerometer can work as a orientation meter in the late interval of mid stance, because the shank is moving with small rotational velocity and acceleration, and the accelerometer is near from rocker (the distance D between accelerometer and ankle joint is about 50 mm). (c) Angular orientations from gyroscope and accelerometer. The intelligent calibrations are implemented through resetting initial value in the integral calculation of gyroscope signal, in which the orientations from accelerometer is used to provide the integral initial value (13).

Table 3
RMSE of orientation drift from integral calculation.

Stride	1	2	3	4
Time (s)	2.45	3.68	4.90	6.26
θ_s (°)	−1.50	−0.28	−0.20	−0.71
θ_s^m (°)	−1.11	1.75	1.24	5.06

θ_s: Shank angle calculated from signal of gyroscope using integral computing (9).
θ_s^m: Shank angle from signal of accelerometer using (13).

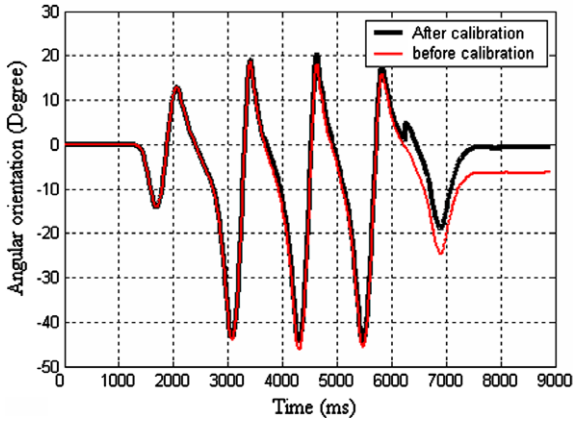

Fig. 12. Period calibration by fusing signals of gyroscopes and accelerometers.

errors are never accumulated with increasing strides, when the calibration was implemented by fusing data of gyroscopes and accelerometers. A set of example comparison figures from verification experiments on segmental angular displacements measured by wearable sensor systems and optical motion analysis systems (Hi-DCam) is given in Fig. 13, which demonstrate the two systems' measurement results have high consistence. Moreover,

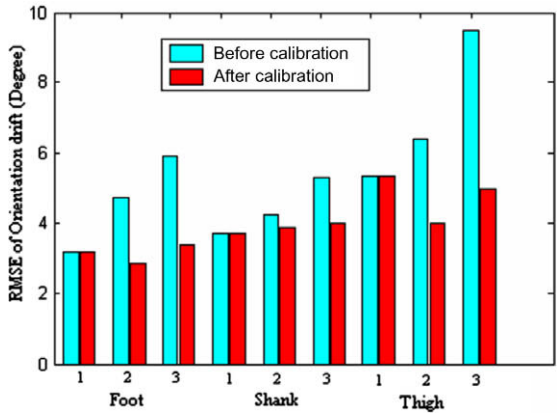

Fig. 14. Average orientation error (RMSE value) using intelligent calibration. In the serial three strides the drift of the three segments (foot, shank and thigh) continuously increases when using direct integral calculation from gyroscope signals. The drift errors are never accumulated with increasing strides, when the calibration is implemented by fusing data of gyroscopes and accelerometers.

Fig. 14 provides a statistical result about the validity of the intelligent calibration for decreasing drift, and experiments were completed on the ten healthy subjects. The average RMSE was not over 5.0° (the thigh angle orientation) when the calibration is implemented. Correlation coefficient (R) was not under 0.9 for the segment angles from the wearable sensor system and the results from the optical motion analysis system.

5. Discussions and conclusions

Quantitative human motion analysis was implemented using a developed wearable sensor system with intelligent calibration. The results from the sensor system showed a high correlation to the results from the optical motion analysis system in the multi-step walking experiments,

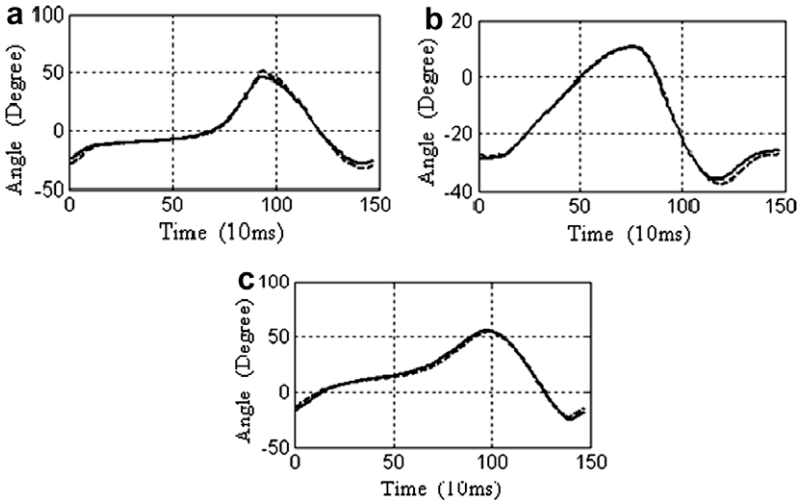

Fig. 13. Segmental angular displacements measured by wearable sensor systems (solid line) and Hi-DCam camera systems (dashed line). (a) Foot angular displacements. (b) Shank angular displacements. (c) Thigh angular displacements.

which proved the validity of the intelligent calibration method for decreasing drift errors.

Pappas et al. [19] described a gait phase detection system which can be used in gait analysis applications and to control gait cycle of a neuroprosthesis for walking, but this system was only designed to detect in real time the following gait phases: *stance*, *heel-off*, *swing*, and *heel-strike*. This kind of gait phase detection often failed to accommodate the gait deviations of patients impaired by paralysis or arthritis whose heel may never contact the ground or do so much later in a gait cycle. In this paper, a normal walking gait cycle is divided into eight gait phases: initial contact, loading response, mid stance, terminal stance, pre-swing, initial swing, mid swing and terminal swing from the generic terminology developed by the Rancho Los Amigos gait analysis committee. We detected the eight gait phases using leg segments orientation angles and the signals of gyroscopes.

The muscular tensions are very complex during walking, and the electromyogram (EMG) is a common method for this study. In next step of this study, we want to develop a wearable sensor system for estimating muscular tensions instead of EMG. Analysis of human walking pattern by the eight gait phases more directly identifies the functional significance (muscular tensions) of the different motions accruing at the individual joints and segments. For example, in mid stance phase including early interval and late interval, the early interval has body over mid foot, in which quadriceps and soleus muscles are in activity; later interval has body over forefoot, in which soleus and gastrocnemius are only extensor muscles around tibia. We can combine the developed wearable human motion analysis sensor system with a reaction force sensor worn under foot to estimate muscular tensions. The gait phase division will improve the precision of this method by providing constrain condition about the functional muscles for an optimum analysis [35,36]. Moreover, in the study of robotics, this wearable sensor system is applied for real-time control of a humanoid robot which may walk in the same phase as human walking.

References

[1] I.A. Karaulova, P.M. Hall, A.D. Marshall, Tracking people in three dimensions using a hierarchical model, Image and Vision Computing 20 (2002) 691–700.

[2] Y. Inoue, T. Matsuda, K. Shibata, Estimation of vertical reaction force and ankle joint moment by using plantar pressure sensor, in: JSME Symposium on Human Dynamics, 2003, pp. 57–62.

[3] W.Y. Wong, M.S. Wong, K.H. Lo, Clinical applications of sensors for human posture and movement analysis: a review, Prosthetics and Orthotics International 31 (2007) 62–75.

[4] H. Zheng, N.D. Black, N.D. Harris, Position-sensing technologies for movement analysis in stroke rehabilitation, Medical and Biological Engineering and Computing 43 (4) (2005) 413–420.

[5] K. Turcot, R. Aissaoui, K. Boivin, M. Pelletier, N. Hagemeister, J.A. De Guise, New accelerometric method to discriminate between asymptomatic subjects and patients with medial knee osteoarthritis during 3-D gait, IEEE Transactions on Biomedical Engineering 55 (4) (2008) 1415–1422.

[6] A. Zijlstra, J.H.M. Goosen, C.C.P.M. Verheyen, W. Zijlstra, A body-fixed-sensor based analysis of compensatory trunk movements during unconstrained walking, Gait and Posture 27 (1) (2008) 164–167.

[7] A.K. Bourke, G.M. Lyons, A threshold-based fall-detection algorithm using a bi-axial gyroscope sensor, Medical Engineering and Physics 30 (1) (2008) 84–90.

[8] J. Favre, F. Luthi, B.M. Jolles, O. Siegrist, B. Najafi, K. Aminian, A new ambulatory system for comparative evaluation of the three-dimensional knee kinematics, applied to anterior cruciate ligament injuries, Knee Surgery, Sports Traumatology, Arthroscopy 14 (7) (2006) 592–604.

[9] K. Aminian, B. Najafi, Capturing human motion using body-fixed sensors: outdoor measurement and clinical applications, Computer Animation and Virtual Worlds 15 (2) (2004) 79–94.

[10] J.J. Kavanagh, H.B. Menz, Accelerometry: a technique for quantifying movement patterns during walking, Gait and Posture 28 (1) (2008) 1–15.

[11] A.M. Sabatini, C. Martelloni, S. Scapellato, F. Cavallo, Assessment of walking features from foot inertial sensing, IEEE Transactions on Biomedical Engineering 52 (3) (2005) 486–494.

[12] K. Aminian, B. Najafi, C. Bula, P.-F. Leyvraz, Ph. Robert, Spatio-temporal parameters of gait measured by an ambulatory system using miniature gyroscopes, Journal of Biomechanics 35 (5) (2002) 689–699.

[13] B. Coley, B. Najafi, A. Paraschiv-Ionescu, K. Aminian, Stair climbing detection during daily physical activity using a miniature gyroscope, Gait and Posture 22 (4) (2005) 287–294.

[14] H.-Y. Lau, K.-Y. Tong, H. Zhu, Support vector machine for classification of walking conditions using miniature kinematic sensors, Medical and Biological Engineering and Computing 46 (6) (2008) 563–573.

[15] B. Najafi, K. Aminian, F. Loew, Y. Blanc, P.A. Robert, Measurement of stand-sit and sit-stand transitions using a miniature gyroscope and its application in fall risk evaluation in the elderly, IEEE Transactions on Biomedical Engineering 49 (8) (2002) 843–851.

[16] K. Aminian, Ph. Robert, E.E. Buchser, B. Rutschmann, D. Hayoz, M. Depairon, Physical activity monitoring based on accelerometry: validation and comparison with video observation, Medical and Biological Engineering and Computing 37 (3) (1999) 304–308.

[17] H. Lau, K. Tong, The reliability of using accelerometer and gyroscope for gait event identification on persons with dropped foot, Gait and Posture 27 (2) (2008) 248–257.

[18] I.P.I. Pappas, T. Keller, S. Mangold, M.R. Popovic, V. Dietz, M. Morari, A reliable gyroscope-based gait-phase detection sensor embedded in a shoe insole, IEEE Sensors Journal 4 (2) (2004) 268–274.

[19] I.P.I. Pappas, M.R. Popovic, T. Keller, V. Dietz, M. Morari, A reliable gait phase detection system, IEEE Transactions on Neural Systems and Rehabilitation Engineering 9 (2) (2001) 113–125.

[20] J.M. Jasiewicz, J.H.J. Allum, J.W. Middleton, A. Barriskill, P. Condie, B. Purcell, R.C.T. Li, Gait event detection using linear accelerometers or angular velocity transducers in able-bodied and spinal-cord injured individuals, Gait and Posture 24 (4) (2006) 502–509.

[21] Available from: <http://www.xsens.com/en/home.php/>.

[22] H. Dejnabadi, B.M. Jolles, K. Aminian, A new approach to accurate measurement of uniaxial joint angles based on a combination of accelerometers and gyroscopes, IEEE Transactions on Biomedical Engineering 52 (8) (2005) 1478–1484.

[23] R. Williamson, B.J. Andrews, Detecting absolute human knee angle and angular velocity using accelerometers and rate gyroscopes, Medical and Biological Engineering and Computing 39 (3) (2001) 294–302.

[24] J. Favre, B.M. Jolles, R. Aissaoui, K. Aminian, Ambulatory measurement of 3D knee joint angle, Journal of Biomechanics 41 (5) (2008) 1029–1035.

[25] R. Zheng, T. Liu, Y. Inoue, K. Shibata, K. Liu, Kinetics analysis of ankle, knee and hip joints using a wearable sensor system, Journal of Biomechanical Science and Engineering 3 (3) (2008) 343–355.

[26] A.M. Sabatini, Quaternion-based strap-down integration method for applications of inertial sensing to gait analysis, Medical and Biological Engineering and Computing 43 (1) (2005) 94–101.

[27] H.J. Luinge, P.H. Veltink, Measuring orientation of human body segments using miniature gyroscopes and accelerometers, Medical and Biological Engineering and Computing 43 (2) (2005) 273–282.

[28] H.J. Luinge, P.H. Veltink, C.T.M. Baten, Ambulatory measurement of arm orientation, Journal of Biomechanics 40 (1) (2007) 78–85.

[29] R.E. Mayagoitia, A.V. Nene, P.H. Veltink, Accelerometer and rate gyroscope measurement of kinematics: an inexpensive alternative to optical motion analysis systems, Journal of Biomechanics 35 (4) (2002) 537–542.

[30] H. Dejnabadi, B.M. Jolles, E. Casanova, P. Fua, K. Aminian, Estimation and visualization of sagittal kinematics of lower limbs orientation using body-fixed sensors, IEEE Transactions on Biomedical Engineering 53 (7) (2006) 1385–1393.

[31] J.Y. Goulermas, D. Howard, C.J. Nester, R.K. Jones, L. Ren, Regression techniques for the prediction of lower limb kinematics, Journal of Biomechanical Engineering 127 (6) (2005) 1020–1024.
[32] A. Findlow, J.Y. Goulermas, C. Nester, D. Howard, L.P.J. Kenney, Predicting lower limb joint kinematics using wearable motion sensors, Gait and Posture 28 (1) (2008) 120–126.
[33] Pathokinesiology Department, Physical Therapy Department: Observational Gait Analysis Handbook, CA, The Professional Staff Association of Rancho Los Amigos Medical Center, 1989.
[34] J. Parry, Gait Analysis Normal and Pathological Function, Slack Incorporated, 1992.
[35] A. Pedotti, V.V. Krishnan, L. Stark, Optimization of muscle-force sequencing in human locomotion, Mathematical Biosciences 38 (1978) 57–76.
[36] Y. Ehara, M. Beppu, S. Nomura, Y. Kunimi, Estimation of energy consumption during level walking, Biomechanisms 10 (1990) 163–172.